Oxygen Reduction on Mild steel - Influence of 2-Carboxy ethyl phosphonate

J.Mathiyarasu and N.Palaniswamy

Corrosion Science and Engineering Division, Central Electrochemical Research Institute, KARAIKUDI - 630 006

Oxygen reduction on mild steel in 100 ppm NaCl solution shows an inhomogeneous, porous, passive film formed on the surface in presence of 2-CEPA + Zn^{2+}. A mechanism of reduction is proposed.

Corrosion of mild steel involves oxygen reduction reaction at cathodic sites, the products being H_2O_2 or OH^- ions [1,2]. Oxygen plays a key role in the corrosion of mild steel in aerated aqueous solutions. Anodic dissolution mainly generates Fe^{2+} ions [3]. In neutral and alkaline solutions, the above reactions result in various kinds of oxo and hydroxo layers containing both Fe^{2+} and Fe^{3+} species. Presence of a thin oxide layer on the metal alters the characteristics of the electron transfer process; rate constant may decrease by several orders of magnitude [4-7]. Depending on the properties of the layers, they can serve as the sites of oxygen / peroxide reduction.

Calvo and Schiffrin studied the electrochemical reduction and catalytic decomposition of H_2O_2 on passive iron; kinetics of this reaction was found to be first order *wrt* peroxide but -1 *wrt* OH^- [8]. The negative reaction order in the latter case was said to indicate an equilibrium process on the passive film prior to electron transfer.

Zecevic *et.al.* [2] studied the reduction of H_2O_2 on iron in the pH range 8.6 - 13.8 in unbuffered & also borate buffers. They found that the reduction is faster at less oxidised surfaces; first electron transfer to molecular H_2O_2 being the rate determining step. The reaction order is found to be 1 *wrt* H_2O_2. Chloride ions excerted no influence on this reduction.

Gojkovic *et.al.* [3] studied the oxygen reduction on iron in both unbuffered and borate buffer solutions of pH 7.4 - 13.8. They reported reaction order *wrt* oxygen as 1. Reaction order *wrt* OH^- depended on pH; it was -1 at pH > 11 and 0 at pH < 11. Adsorption of O_2 molecule on $Fe(II)_{ads}$ active site was proposed as the rate determining step in both mechamisms.

Based on the electrical impedance behaviour of iron in neutral aqueous phosphonate solution, Rammelt *et.al.* [9] observed that phosphonate partially blocked the metal surface leading to an inhomogeneous transport impedance; but phosphate coated layer formed a more or less homogeneous layer slowing down the mass transport rate.

Juttner and coworkers [10] interpreted the impedance spectra of corroding carbon steel surfaces by assuming that partially blocked surface can be considered to consist of an array of inactive hexagons of latteral size 'r' each one containing a

© E.C.S.I. Bangalore

circular active area of radius 'a' [11]. Both anodic dissolution of iron (mainly charge transfer controlled) and reduction of oxygen (diffusion controlled) take place on the active sites.

The present work looks into the kinetics and mechanism of oxygen reduction on mild steel in near neutral solution containing 100 ppm NaCl with and without inhibitor (2-carboxyethyl phosphonate complex - 2-CEPA + Zn^{2+}). The reaction was studied at a rotating disc electrode using potentiostatic polarisation and electrochemical impedance spectroscopy.

EXPERIMENTAL

The composition of the mild steel electrode was 0.02 - 0.03% S, 0.3 - 0.8% P, 0.4 - 0.5% Mn, 0.1 - 0.2% C and rest iron. The experiments were carried out in a three electrode (mild steel, Pt, SCE) glass cell. The mild steel rotating disc working electrode was polished with emery paper 1/0 to 4/0 grit and successively rinsed with distilled water followed by trichloroethylene. The polarisation curves (E *vs* i) were obtained in the potential range -300 to -1400 mV and a potential sweep rate of 1.0 mV/sec. Bi-potentiostat (PAR Model 366) was used for this purpose. Runs were repeated to ensure reproducibility.

Impedance measurements were made in the frequency range 10 mHz to 10 kHz (moving from high frequency towards lower) using an A.C.impedance system (PAR Model 6310). Impedance spectra were taken at different potentials.

All the solutions were prepared with triple distilled water and analytical grade chemicals. Solutions were oxygen saturated prior to each experiment. All experiments were carried out at room temperature (25±2°C).

RESULTS

Polarisation Studies

Polarisation curves for oxygen reduction on mild steel in 100 ppm NaCl solution is shown in Fig 1 (a - without any additive and b- with addition of 2-CEPA + Zn^{2+}). In the inhibitor - free system, (Fig.1A) the curves do not show well defined limiting region at any rotational speed, but a limiting current region is seen at high negative potentials in presence of the inhibitor system (Fig.1B.

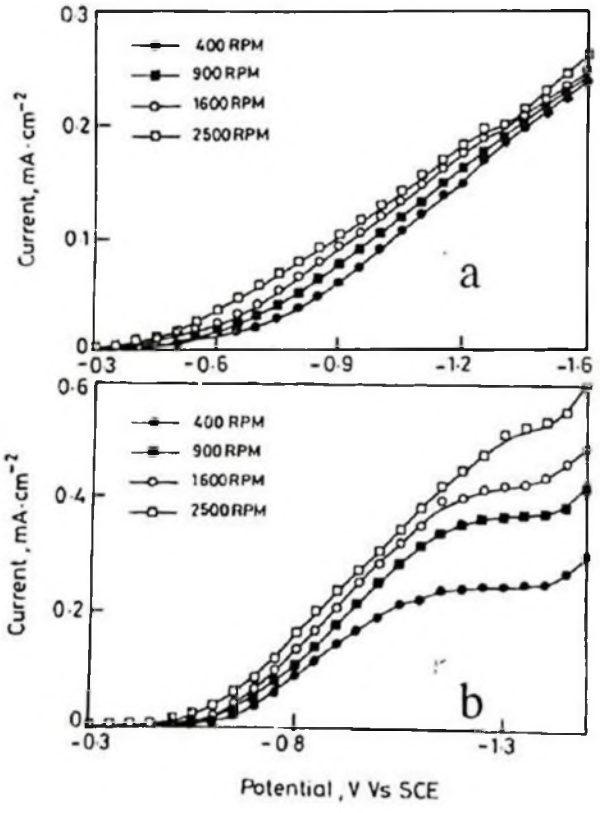


Fig.1 Polarisation curves for O_2 reduction on mild steel at various rotation rates.
a) in 100 ppm NaCl solution
b) in 100 ppm NaCl solution in presence of 2-CEPA and Zn^{2+} ion

The reaction order *wrt* oxygen was determined from the slope of the plot:

$$\log i = \log i_k + m \log (1 - i/i_l) \quad \ldots \quad (1)$$

where i and i_l are the current and limiting current measured at the same rotation speed, m is the reaction order and i_k is the current density corrected for diffusional effects, i.e. kinetic current density. Values of i and i_l are taken from polarisation curves (Fig 1). The linear plots are shown in Fig 2. The slope values (the reaction order) are found to be close to 1 at all potentials in the region -0.8 to -1.2 V indicating the reaction to be of first order at potentials more negative than -0.7 V.

In order to obtain Tafel plots for processes under mixed (activation - diffusion) control, the value of kinetic current (i_k) has to be determined at each potential. This value has been determined from the intercept of the linear plot of equation (Fig 2.) However, this value is the coverage value for several rotation rates.

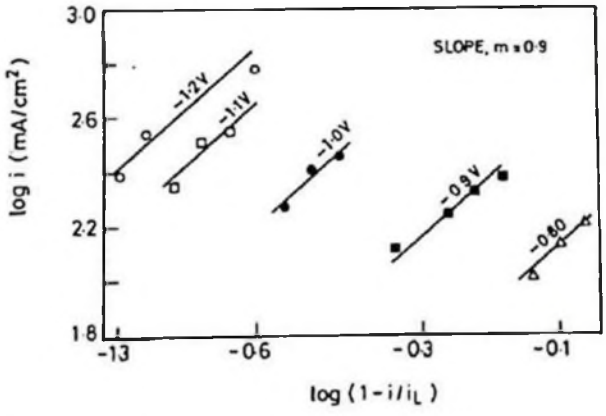


Fig.2 Reaction order at various potentials on Mild steel
Medium 100 ppm NaCl with 2-CEPA and Zn^{2+} ion

A value of i_k, at a given potential at a specified speed of rotation, can be determined as follows: Since the value of the slope m is nearly 1 in Fig 2, the equation 1 can be rewritten as

$$i_k = \frac{i \cdot i_l}{i_l - i} \qquad \ldots (2)$$

where i_l is the limiting current. The measured currents can be corrected for diffusion effects by using this equation.

The Tafel slopes for oxygen reduction on mild steel using the i_k value by both the methods are presented in Fig 3. Slope value is found to be -68 mV for inhibitor system (2CEPA + Zn^{2+} ion) in 100 ppm NaCl solution.

For the first order reaction, the measured reduction current i is related to rotation speed , by the expression:

$$1/i = 1/i_k + (1/B)\ \omega^{-1/2} \qquad \ldots (2)$$

where i_k is the kinetic current density and 'B' is the Levich slope [12].

A plot of 1/i *vs* $\omega^{-1/2}$ (from the data taken from Fig 1a,b) are shown in Fig 4a,b. The Levich Slope values (B) are found to decrease as the potential becomes more negative. The significant change of B with potential is in fact related to the time dependence of the concentration of active species

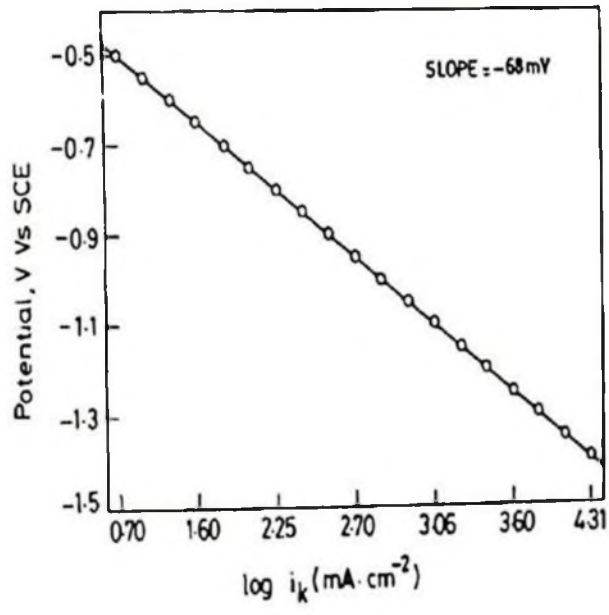


Fig.3 Tafel plots for the O_2 reduction on Mild Steel

Medium 100 ppm NaCl with 2 CEPA and Zn^{2+} ion. Rotation rate 1600 rpm: (i_k calculated using equation 2).

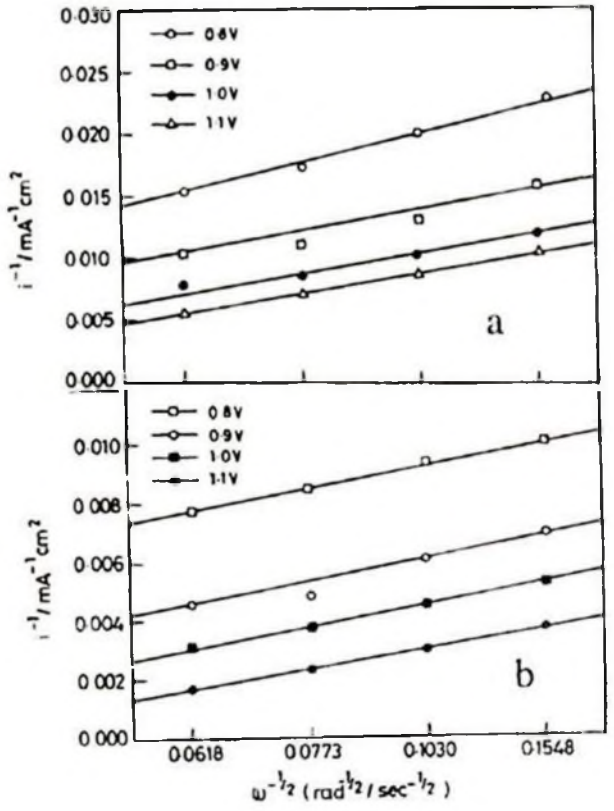


Fig.4 1/i *vs* $\omega^{-1/2}$ plots for the O_2 reduction on mild steel at various potentials.

a) in 100 ppm NaCl solution
b) in 100 ppm NaCl solution in presence of 2-CEPA and Zn^{2+} ion
Data taken from Fig 1a & 1b.

which is being consumed during successive measurements at different potentials.

Electrochemical Impedance Spectral Studies

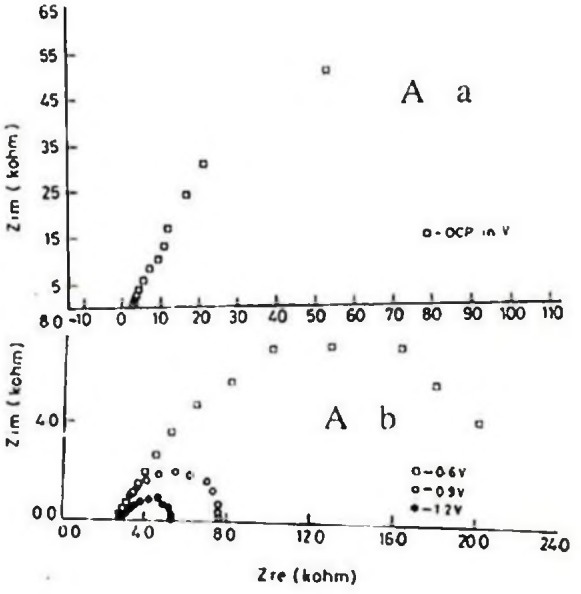
The Nyquist plots of the EIS spectra of mild steel obtained in aerated medium are shown in Figs 5 A&B. The film resistance (R_f) calculated from the plots are listed in Table 1.

At -300 mV, it is difficult to find out the R_f values, since it gives a rising curve rather than a semicircle. In other cases, the value of the system containing 100 ppm NaCl is found to decrease as the potential moves in the negative direction.

Double layer capcitance value (C_{dl}) given in the Table 1 is calculated from ω_{max} using the following equation [13].

$$C_{dl} = \frac{1}{\omega_{max} \cdot R_f}$$

$\omega_{max} = 2\ \pi\ f_{max}$ where f_{max} is the corresponding frequency of the impedance at the apex of the



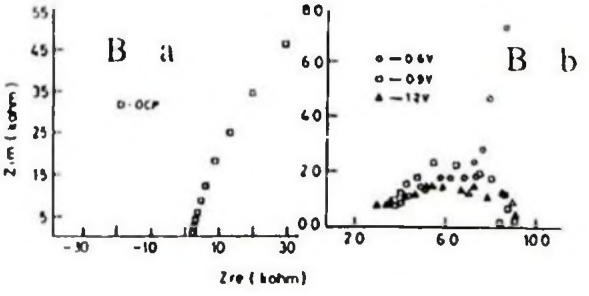


Fig.5 Nyquist Plots of Mild Steel at various Potentials

Rotation speed 1600 rpm
A. Medium oxygenated 100 ppm NaCl solution
B. oxygenated 100 ppm NaCl solution with CEPA and Zn^{2+} ion

Table 1

Parameters Derived from the Nyquist Plots (Fig 5)

Specimen: Mild steel Medium : Oxygenated Neutral Aqueous : Rotation Speed 1600 RPM

Potential mV	R_s kOhm.cm^2	R_t kOhm.cm^2	R_f kOhm.cm^2	f_{max} Hz	C_{dl} µFcm^{-2}
In 100 ppm NaCl					
-300	1.034	-	-	-	-
-600	0.979	20.03	19.05	0.398	20.99
-900	1.026	7.66	6.63	1.585	15.14
-1200	1.879	5.37	3.49	1.585	20.77
In 100 ppm NaCl + 2 CEPA + Zn^{2+}					
-300	0.804	-	-	-	-
-600	1.127	9.06	7.93	6.310	3.18
-900	1.118	12.31	11.19	-	-
-1200	0.796	9.09	8.29	2.512	7.64

semicircle of the Nyquist plots. At all potentials, the one corresponding to the low frequency range, is due to mass transfer and the loop corresponding to the high frequency range is ascribed to the combination of charge transfer resistance and double layer capacitance.

DISCUSSION

Polarisation Behaviour

Earlier work [14] has shown that 2-CEPA alone has low inhibitive action (efficiency < 5%) for mild steel in neutral aqueous medium. But with the addition of Zn^{2+} ions, the inhibition efficiency has increased many fold.

Polarisation curves in inhibitor - free solution do not give a defined limiting current region (Fig.1a). Hence, it is difficult to find out the order and Tafel slope for this particular system. Impedance spectra at various potentials with constant rotation speed (Fig. 5) have shown that the redox reaction is under diffusion control at -300 mV but, the reaction is under fully activation or charge transfer control at high negative potentials. Table 1 shows that the R_t values decrease with increase in potential thus leading to an enhanced activation process at the electrode interface. At low negative potential, coverage of oxide film on the electrode surface makes the reaction to be under diffusion control. At more negative potential, the hydrogen evolution disturbs the oxide film and therefore the reaction becomes fully under charge transfer control.

Polarisation curves in presence of inhibitor system (2-CEPA + Zn^{2+}) show a clear limiting region (Fig 1b) at higher cathodic potential (-900 mV *vs* SCE). With increase in the rotation speed, the limiting region shifts to the negative direction; the limiting current also increases : (253 mA at 400 rpm and 580 mA at 2500 rpm). The inhibitor

enhances film formation on the surfaces which in turn enhances the oxygen reduction process by surface catalytic activity. The reaction order is found to be close to 1 (Fig.2); the reaction kinetics is of the first order with respect to dissolved oxygen.

Tafel slope is found to be -68 mV. $dec.^{-1}$ (Fig.3). Gerisher and Gerisher [15] have reported a Tafel slope of about -280 $mV.dec^{-1}$ and Huang *et. al.* [16] reported a value of -200 $mV.dec^{-1}$ for H_2O_2 reduction at Pt in acid solutions. A high Tafel value was also observed for H_2O_2 reduction on Au in dilute acid solutions [17]. They describe the high slopes (upto 300 $mV.dec^{-1}$) as due to metallic conductivity of the electrode surface. The low Tafel slope (-68 $mV.dec^{-1}$) points to the significant influence of the inhibitor film on the oxygen reduction reaction. In the present system, the low value can be attributed to the low/semi conducting property of the inhibitor complex formed on the electrode surface.

The changes in the surface film occurs with potential simultaneously with oxygen reduction, one can say that the real cathode transfer coefficient is α 1. This can be due to the adsorption of intermediates under Temkin conditions or due to an electro-chemical reaction mechanism in which a fast electrochemical step is followed by a slow chemical step.

The most probable constituents of the oxide film, (γ-Fe_2O_3 and γ-FeOOH) can behave like n-type semiconductor or insulator [18]. However, the oxide film is very thin (about 3 nm) and the whole concept of semiconductor behaviour for such a thin film is questionable. So the low Tafel value cannot be attributed to the semi conducting behaviour of the film on the electode. One can only conclude that the complex reactive mechanism is responsible for the low Tafel slope.

EIS Spectra

EIS spectra (Fig. 5) show that at -300 mV no semicircle is observed. At this potential the electro active species diffuses through the pores of surface film to undergo reduction. The absence of the semi circle could be due to uneven frequency distribution around the curve.

The nature of the Nyquist plot, at -600 mV shows the O_2 reduction reaction occuring on the surface on the adsorbed layer of the inhibitor complex over the oxide film layer. At higher potential (-900 mV), a high frequency semicircle followed by a rising Warburg diffusion impedance tail at low frequency observed can be explained as due to reduction under charge transfer control at higher frequencies followed by a diffusion control at low frequency. At -1200 mV the distorted semicircle explains that the reaction is either under charge transfer or activation control.

Based on the above discussion, the following sequence is visualised. A semi-conducting film formed by the inhibitor mixture is adsorbed over the oxide film and the O_2 reduction reaction takes place over this. From the Nyquist curves, it is observed that the O_2 reduction reaction got suppressed at higher potentials by the inhibitor film. But at the higher potentials the R_f values were found to be more or less same; the O_2 - reduction reaction seems to be enhanced by the surface film which acts as a catalytic surface. So the higher impedance part is related to the C_{dl} in parallel with the R_f whilst the low frequency part can be attributed to a diffusion impedance. Under diffusion control, the Warburg coefficient σ_D is

indicative of the diffusion rate of the reacting species [9]. The diffusion impedance is caused by the transport of O_2 within the pores of the inhibitor film to the metal surface. Hence, the diffusion impedance is independent of the rotation speed and disappears in the absence of O_2.

Reaction Mechanism

The reduction of O_2 in aqueous solution occurs by several possible pathways [18,19]. The reduction can occur

(a) by a direct 4e⁻ addition giving H_2O (in acid) or OH^- (in alkaline)
(b) by a 2e⁻ addition to adsorbed H_2O_2 (in acid) or to adsorbed HO_2^- (in alkaline). This may be followed by desorption of H_2O_2 species and its accumulation in solution.
(c) by direct 4e⁻ reduction and a 2e⁻ reduction.
(d) by a 2e⁻ reduction with further reduction of the H_2O_2 formed.
(e) by a direct 4e⁻ reduction coupled to the series of reduction.

The O_2 reduction in near neutral solution may be given as follows:

$$O_2 \longrightarrow O_2 \text{ (ads)}$$
$$O_2 \text{ (ads)} + e^- + H_2O \longrightarrow O_2H \text{ (ads)} + OH^-$$
$$O_2H \text{ (ads)} + e^- \rightleftharpoons O_2H^-$$
$$O_2H^- + H_2O \longrightarrow H_2O_2 + OH^-$$

On the basis of the above, the mechanism of O_2 reduction with an addition of 2CEPA + Zn^{2+} ion on mild steel may be described as follows:

In inhibitor free system, the redox process takes place over the oxide layer of mild steel and the formation of O_2H^- is the rate determining step. In presence of inhibitor, the redox process takes place

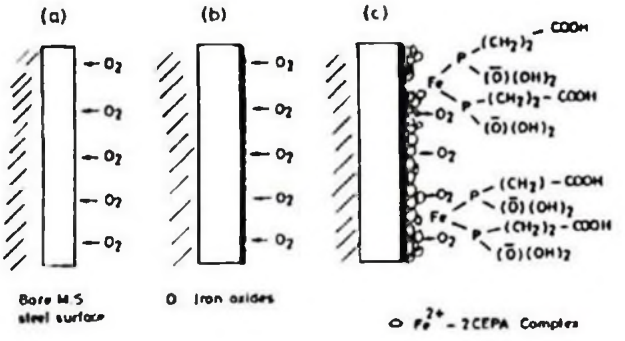


Fig.6 Schematic diagram to illustrate the various diffusion processes that may be occuring during O_2 reduction on mild steel.

a. Surface without any coverage
b. Surface with oxide coverage
c. Surface with oxide as well as inhibitor complex coverage

over a surface of a passive semiconducting inhibitor film. Here it is worth mentioning that the film formed by inhibitor complex is porous in nature and it enhances the O_2 - reduction due to its catalytic activity.

In the proposed model (Fig.6), no specific mention has been made regarding the possible semiconducting properties of inhibitor film. However, Gunasekaran *et. al*, [14] in their earlier work pointed out that the inhibitive protective film has semiconducting properties. Therefore the electrochemical (ECE) mechanism based on the ideas of the redox surface catalyst advanced by Beck [20] where the H_2O_2 reduction is mediated by surface Fe^{2+} centres [8] is quite possible and cannot be ruled out on the basis of chloride ion adsorption. It should be pointed out that the reaction mechanism with the first electron transfer O_2 molecule to be fast, (which is the rate determining step) is quite unusual for O_2 reduction on substrate other than passive iron. This hypothesis is based on the assumption that $\alpha = 1$. However, the apparent transfer coefficient observed experimentally lies between 0.5 and 1. Therefore one cannot say for

sure that the proposed mechanism is correct unless the higher 'a' value is explained by the simultaneous change of composition and structure of the passive film.

CONCLUSIONS

The following conclusions are drawn from the experimental results:

1. The O_2-reduction on mild steel in the presence of 2CEPA + Zn^{2+} ion proceeds with the reaction order of 1 with respect to O_2. The Tafel slope is about -68 $mV.dec^{-1}$.
2. The O_2 reduction reaction takes place on the inhibitor layer which is adsorbed on the oxide layer of the metal surface.
3. The inhibitor layer is found to be inhomogenious or porous in nature and it enhances the O_2 - reduction process because of its catalytic activity.

ACKNOWLEDGEMENT

The authors thank the Director, Central Electrochemical Research Institute, Karaikudi for his kind permission to publish this paper. One of the authors (J.M) thanks the Council of Scientific and Industrial Research, New Delhi, for the award of a Fellowship.

REFERENCES

1. V.Jovancicevic and J.O'M.Bockris, *J.Electrochem.Soc.*, **133** (1986) 1797.
2. S.Zecevic, D.M.Drazic and S.Gojkovic, *J.Electroanal.Chem.*, **265** (1989) 179.
3. S.Lj.Gojkovic, S.K.Zecevic and D.M.Drazic, *Electrochim. Acta*, **39** (1994) 975.
4. R.V.Moshtev, *Electrochim. Acta*, **16** (1971) 2039.
5. A.M.T.Olmedo, R.Perreiro and D.J.Schiffrin, *J. Electroanal. Chem.*, **74** (1976) 19.
6. M.Frazak and Trinh Zung Sen, *Electrochim. Acta*, **21** (1976) 509.
7. J.W.Schultze and U.Stimming, *Z.Phys.Chem. N.F.*, **98** (1975) 285; U.Stimming and F.W.Schultze, *Electrochim. Acta*, **24** (1979) 859
8. E.J.Calvo and D.J.Schiffrin, *J. Electroanal. Chem.*, **163** (1984) 257.
9. U.Rammelt and G.Reinhard, *Electrochim. Acta*, **40** (1995) 505.
10. K.Juttner, W.J.Lorenz, M.W.Kendig and F.Mansfeld, *J. Electrochem. Soc.*, **135** (1988) 332; E.Schmidt, J.Hitzig, J.Titz, K.Juttner and W.J.Lorenz, *Electrochim. Acta*, **31** (1986) 1041; J.Hitzig, J.Titz, K.Juttner, W.Z.Lorenz and E.Schmidt, *Electrochim. Acta*, **29** (1984) 287; M.Stieble and K.Juttner, *J. Electroanal. Chem.*, **290** (1990) 163.
11. T.Gueshi, T.Tokuda and H.Matsuda, *J. Electroanal. Chem.*, **89** (1978) 247.
12. V.G.Levich, *Physicochemical Hydrodynamics*, **Prentice Hall, Englewood Cliffs, NJ** (1962).
13. F.Mansfield, *Corrosion, NACE*, **36** (1986) 301.
14. Guruswamy Gunasekaran, N.Palaniswamy and B.V.Apparao, *Bull. Electrochem.* **12** (1996) 59.
15. G.Gerisher and H.Gerisher, *Z. Phys. Chem. N.F.*, **6** (1956) 178.
16. J.C.Huang, R.K.Sen and E.Yeager, *J. Electrochem. Soc.*, **126** (1979) 786.
17. R.W.Zurilla and E.Yeager, *Technical Report No.23, ONR Contract No.N-14-67-C 0389*, **Case Western Reserve University**, Cleveland, OHIO (1969).
18. V.S.Bagotskii, M.R.Taraserich and V.YU.Filinovskii, *Sov. Electrochem.*, **5** (1969) 1158 & **8** (1972) 81; V.Stimming and J.W.Shulze, *Electrochim. Acta*, **24** (1979) 859 and *Ber. Bunsenges. Phys. Chem.*, **80** (1976) 1297.
19. H.S.Wroblowa, Yen-Chi-pan and G.Razumneg, *J. Electroanal. Chem.*, **69** (1986) 195.
20. F.Beck, *J. Appl. Electrochem.*, **7** (1977) 239.